

Short communication

# Satellite-derived surface water $p\text{CO}_2$ and air–sea $\text{CO}_2$ fluxes in the northern South China Sea in summer

Yu Zhu, Shaoling Shang<sup>\*</sup>, Weidong Zhai, Minhan Dai

State Key Laboratory of Marine Environmental Science, Xiamen University, Xiamen 361005, China

Received 6 May 2008; received in revised form 23 July 2008; accepted 17 September 2008

## Abstract

An empirical approach is presented for the estimation of the partial pressure of carbon dioxide ( $p\text{CO}_2$ ) and air–sea  $\text{CO}_2$  fluxes in the northern South China Sea in summer using satellite-derived sea surface temperatures (SSTs), chlorophyll-*a* (Chl *a*) concentrations, and wind fields. Two algorithms were tested. The first used an SST-dependent equation, and the other involved the introduction of Chl *a*. Regression equations were developed for summer based on *in situ* data obtained in July, 2004. Using the monthly average SST and Chl *a* fields derived from the advanced very high resolution radiometer (AVHRR) and the SeaWiFS (sea-viewing wide field of view sensor), respectively, the monthly  $p\text{CO}_2$  fields were computed. The derived  $p\text{CO}_2$  was compared with the shipboard  $p\text{CO}_2$  observations conducted in July, 2000. This resulted in a root-mean-square error of 4.6  $\mu\text{atm}$ , suggesting that the satellite-derived  $p\text{CO}_2$  was in general agreement with the *in situ* observations. The air–sea  $\text{CO}_2$  flux was further computed with the aid of the monthly mean QuikSCAT wind speed. We contend that more shipboard data are necessary for refining the empirical algorithms and reducing the uncertainty in the results.

© 2009 National Natural Science Foundation of China and Chinese Academy of Sciences. Published by Elsevier Limited and Science in China Press. All rights reserved.

**Keywords:**  $p\text{CO}_2$ ; Remote-sensing; Northern South China Sea;  $\text{CO}_2$  flux

## 1. Introduction

Accurate estimation of the air–sea  $\text{CO}_2$  fluxes is essential for the study of global carbon cycling and climate change. Until now, estimation of air–sea  $\text{CO}_2$  fluxes has been made based on shipboard (research vessels) measurements of the air and sea surface  $p\text{CO}_2$ . This obviously results in limitations in terms of spatial and temporal coverage.

Sea surface  $p\text{CO}_2$  depends largely on the sea surface temperature (SST). When the SST increases by 1 °C, the surface  $p\text{CO}_2$  increases by 4% [1]. The primary productivity in the upper ocean is also a key factor associated with the surface  $p\text{CO}_2$  [2,3]. Therefore, there is potential to

remotely sense the surface  $p\text{CO}_2$  using satellite data based on its correlation with SST, Chl *a* and other key parameters. This has resulted in the development of empirical algorithms for satellite-derived  $p\text{CO}_2$ . Various algorithms have been derived for different areas of different spatial scales. In the north Pacific, Stephens et al. attempted to study the distribution of  $p\text{CO}_2$  using remote-sensing SST data [4]. Ono et al. then introduced Chl *a* as an additional regression parameter and obtained the reduced root-mean-square (RMS) error [2]. Sarma et al. further developed a remote-sensing algorithm for  $p\text{CO}_2$ , which contained three parameters (SST, Chl *a* and climatological salinity) [5]. Lohrenz and Cai added chromophoric dissolved organic matter (CDOM) as a parameter in their remote-sensing algorithm for  $p\text{CO}_2$ , based on the fact that a good correlation existed between CDOM and salinity in the Mississippi plume [3].

<sup>\*</sup> Corresponding author. Tel.: +86 592 2184781; fax: +86 592 2188071.  
E-mail address: [sishang@xmu.edu.cn](mailto:sishang@xmu.edu.cn) (S. Shang).

The South China Sea (SCS) is one of the world's major marginal seas. The recent field observations suggest that the SCS is a source of atmospheric CO<sub>2</sub> [6,7]. The development of a regional *p*CO<sub>2</sub> remote-sensing algorithm for the SCS would greatly improve the spatial coverage of *p*CO<sub>2</sub> observations. This paper attempts to develop a *p*CO<sub>2</sub> remote-sensing algorithm for the northern SCS, based on regional *in situ* data. The performance of different algorithms was examined by comparing an algorithm based on one single variable SST with another algorithm based on both SST and Chl *a*. The better one was then adopted for estimating the regional air–sea CO<sub>2</sub> fluxes.

## 2. Data sources

### 2.1. Field data

*In situ* data of *p*CO<sub>2</sub> obtained in the northern SCS during July 11–22, 2004 were used for tuning the algorithm (Fig. 1a). Another independent *p*CO<sub>2</sub> dataset, collected from July 19–21, 2000, was used for validation. The *in situ* surface water *p*CO<sub>2</sub> was determined using an underway system with a continuous flow equilibrator [7]. Synchronous sea surface temperature, conductivity and Chl *a* were measured continuously using a SEACAT thermosalinograph system (CTD, SBE21, Sea-Bird with a WetLab fluorometer mounted) [7].

### 2.2. Remote-sensing data

Monthly average data of AVHRR SST and SeaWiFS Chl *a* were taken from the data center of the NASA JPL (Jet Propulsion Laboratory) (<http://podaac.jpl.nasa.gov>) and the data center of the NASA GSFC (Goddard Space Flight Center) (<http://oceans.gsfc.nasa.gov>), respectively. The spatial resolution was 4 km for the former and 9 km for the latter. QuikSCAT wind field data were also taken from the NASA JPL. The data from the ascending and descending passes were averaged at a spatial resolution of 0.25°. These three datasets within the target region (the northern SCS, 15–24°N, 105–120°E) during 2000–2005 were processed to derive the summer average (June–August) SST, Chl *a* and wind field for each year.

## 3. Algorithms for *p*CO<sub>2</sub> in the northern South China Sea in summer

The number of *p*CO<sub>2</sub> values and the matching SST and Chl *a* data collected in 2004 was 9476. Due to the fact that the current algorithm is not sufficiently reliable to derive Chl *a* in very near-shore and usually turbid waters, we excluded this region by focusing on the northern SCS outer shelf/slope and basin waters. In July, the sea surface salinity in the northern SCS typically lies between 33.5 and 34.0 [8]. A salinity value of 33.5 was thus used as the threshold. Any surface water with a salinity lower than this was categorized as being near-shore water and was excluded. Because the Chl *a* in the shelf water of the SCS is usually lower than 1 mg m<sup>-3</sup>, any value higher than this was also discarded. This filtering process resulted in 6871 groups of data. This dataset included 3034 data points collected at two time-series stations over a period of two days, which accounted for 44% of the total data volume. Statistical fitting was then applied to these data using the software package SigmaPlot.

### 3.1. Algorithm based on a single parameter (SST)

The SST is usually the main controlling factor of *p*CO<sub>2</sub> in open oligotrophic waters [7], which forms a theoretical basis for deriving *p*CO<sub>2</sub> from remote-sensing SSTs. The northern SCS is among the regions of low primary production [9]. As expected, the *p*CO<sub>2</sub> was found to be positively correlated with SST (Fig. 2a). We then obtained the empirical function below:

$$p\text{CO}_2 = 6.34T^2 - 366.65T + 5678.53 \quad (n = 6871, R^2 = 0.66) \quad (1)$$

where *T* is the SST (°C).

### 3.2. Algorithm based on two parameters (SST and Chl *a*)

Fig. 2b shows that the *p*CO<sub>2</sub> in the northern SCS in summer appears to decrease with an increase in Chl *a*, suggesting that the change in *p*CO<sub>2</sub> is also affected by Chl *a*. Due to the involvement of the diurnal fluctuations of phytoplankton metabolisms, the relationship between *p*CO<sub>2</sub>

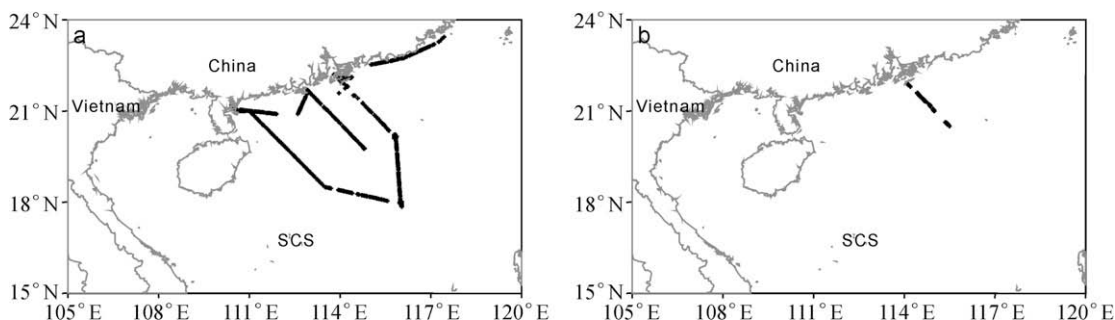


Fig. 1. Cruise tracks for underway measurements in the northern South China Sea. (a) July 11–22, 2004; (b) July 19–21, 2000.

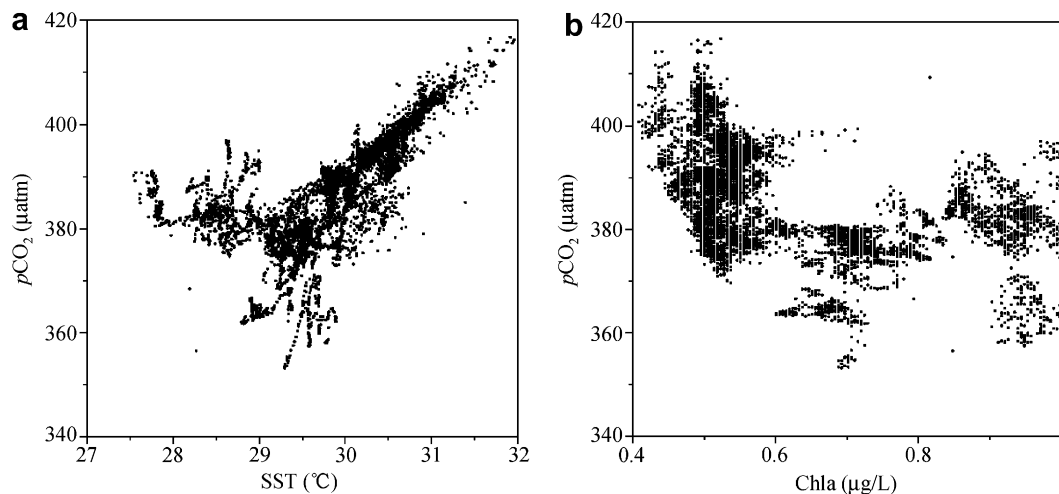


Fig. 2. Correlation between  $p\text{CO}_2$  and SST (a), and between  $p\text{CO}_2$  and Chl  $a$  (b) in the northern South China Sea in July 2004.

and Chl  $a$  failed to turn out as a simple linear function. We therefore adapted the algorithm for the northern SCS to include Chl  $a$ , as shown below:

$$p\text{CO}_2 = 6.31T^2 + 61.9\text{Chl}a^2 - 365.85T - 94.41\text{Chl}a + 5715.94 \quad (n = 6871, R^2 = 0.68) \quad (2)$$

#### 4. Validation of the $p\text{CO}_2$

Satellite-derived  $p\text{CO}_2$  in the northern SCS in July 2000 was computed using the above two algorithms. In order to eliminate the errors induced by the distortion of the remote-sensing Chl  $a$  in very near-shore water, the remote-sensing SST and Chl  $a$  data from the depths of less than 30 m were discarded. Comparisons were then made between the computation results and the field measurements ( $n = 24$ ) in July 2000 (Fig. 3). It is obvious that the results of the two-parameter algorithm showed a better agreement with the measured values than those of the SST-based algorithm. The RMS error of the former was  $4.6 \mu\text{atm}$ , while that of the latter was up to  $25.1 \mu\text{atm}$ . This suggests that the effects of biological activities on the spa-

tial and temporal changes in  $p\text{CO}_2$  in the northern SCS cannot be ignored, and an algorithm dependent on both SST and Chl  $a$  is a better fit for the target region. Further optimization of this algorithm based on a larger pool of *in situ* data is nevertheless advocated. Similarly, a SST-dependent algorithm applied in the oligotrophic subtropical region of the North Pacific resulted in a regression error RMS of  $17 \mu\text{atm}$  [4]. When this algorithm was applied to the relatively productive northwest area of the North Pacific, a much higher regression error RMS of  $40 \mu\text{atm}$  was produced [4]. In contrast, when an algorithm including Chl  $a$  was applied, the regression error RMS decreased to  $\leq 17 \mu\text{atm}$  for both the oligotrophic (the subtropical region,  $20\text{--}43^\circ\text{N}$ ,  $\text{RMS} = 14 \mu\text{atm}$ ) and the productive regions (the subarctic region,  $\text{RMS} = 17 \mu\text{atm}$ ) [2].

It is, nevertheless, obvious that there are significant discrepancies between each pair of data, due mainly to the differences in the time scales of the remote-sensing and the *in situ* data. The remote-sensing data used in this paper were on a monthly scale, while the temporal resolution of the *in situ* data was on the order of minutes. It is clear that relatively drastic short-term changes in  $p\text{CO}_2$ , such as diurnal variations, cannot be reflected in the remote-sensing

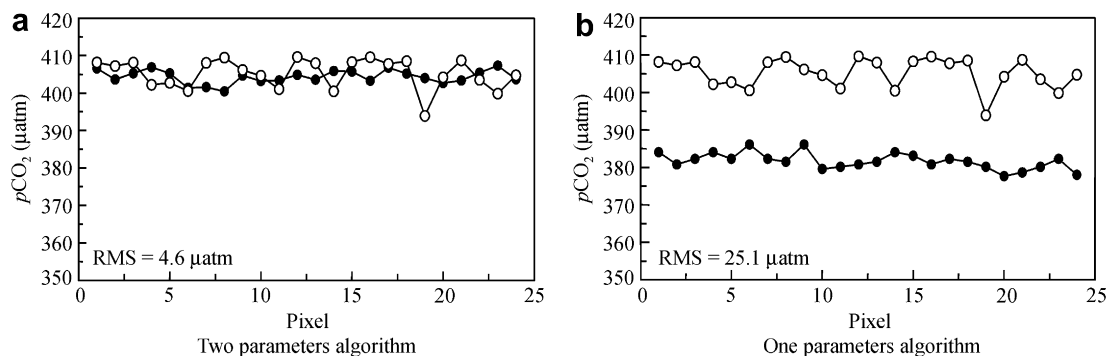


Fig. 3. Comparison between satellite-derived  $p\text{CO}_2$  (—●—) and the *in situ* measured  $p\text{CO}_2$  (---○---) in July 2000; the *in situ* data were spatially averaged to match the low resolution of the satellite-derived data. (a) Results derived from the SST and Chl  $a$ -dependent algorithm; (b) results derived from the SST-dependent algorithm.

data. Nevertheless, we contend that these two data sets from remote-sensing and *in situ* observations complement each other, and the mismatching in time scales between them does not affect the comparison between different algorithms.

## 5. Estimates of air–sea CO<sub>2</sub> fluxes in the northern South China Sea in summer

CO<sub>2</sub> air–sea flux can be estimated as below [10]:

$$F = k \times K_H \times (\Delta p\text{CO}_2)_{\text{sea-air}} \quad (3)$$

where  $F$  is the net air–sea flux of CO<sub>2</sub>;  $(\Delta p\text{CO}_2)_{\text{sea-air}}$  is the sea–air  $p\text{CO}_2$  difference,  $K_H$  is the solubility of CO<sub>2</sub> in seawater [11], and  $k$  is the gas exchange coefficient, which is usually expressed as a function of wind speed. We used the Wanninkhof equation [12] to compute  $k$ :

$$k = f \times u_{10}^2 \times (S_c/660)^{-0.5} \quad (4)$$

where  $S_c$  is the Schmidt number of CO<sub>2</sub> in seawater ( $S = 35$ );  $u_{10}$  is the wind speed at 10 m above sea level derived by QuikSCAT; and  $f$  is a proportional coefficient. When the long-term average wind speed is used,  $f$  equals 0.39, and if instantaneous wind speed is used,  $f$  is 0.31.

Atmospheric  $p\text{CO}_2$  can be computed using the following equation [13]:

$$p\text{CO}_2^{\text{air}} = x\text{CO}_2^{\text{air}}(p_b - p\text{H}_2\text{O}) \quad (5)$$

where  $p_b$  is the air pressure (approximately 1 atm); and  $p\text{H}_2\text{O}$  is the water vapor pressure at the boundary of air and sea observed by AVHRR;  $x\text{CO}_2^{\text{air}}$  is the molar ratio of CO<sub>2</sub> in dry air. For the  $x\text{CO}_2^{\text{air}}$  values, the observations at Mariana Islands (13°6'N, 144°7'E) by the NOAA/Climate Monitoring and Diagnostics Laboratory (CMDL) were used, because they had been found to be close to the historical field measurements in the northern SCS [7].

Satellite-derived  $p\text{CO}_2$  data from the SST and Chl  $a$ -dependent algorithm were then used to estimate the air–sea CO<sub>2</sub> flux in the northern SCS in July 2000. The spatial mean flux was 7.65 mmol CO<sub>2</sub> m<sup>-2</sup> day<sup>-1</sup> from sea to air, quite similar to the field-measured flux (7.50 mmol CO<sub>2</sub> m<sup>-2</sup> day<sup>-1</sup>) [7].

The climatological mean CO<sub>2</sub> flux in summer during the 2000–2005 period in the northern SCS was further estimated (Fig. 4). Again, the data from the depths of ≤30 m were discarded. A distinct spatial pattern of CO<sub>2</sub> flux emerged. The CO<sub>2</sub> flux was higher over the basin water compared with the coastal area, and was higher in the northeastern SCS than in the northwestern SCS. For example, the averaged CO<sub>2</sub> flux offshore of Vietnam and in the Gulf of Tonkin was approximately 3.5 mmol CO<sub>2</sub> m<sup>-2</sup> day<sup>-1</sup>, while it ranged between 7 and 9 mmol CO<sub>2</sub> m<sup>-2</sup> day<sup>-1</sup> in the northeastern SCS. This was more or less associated with the uneven wind field in the northern SCS, as revealed by QuikSCAT. Therefore, the uncertainty would be great if the air–sea CO<sub>2</sub> fluxes in the whole of the

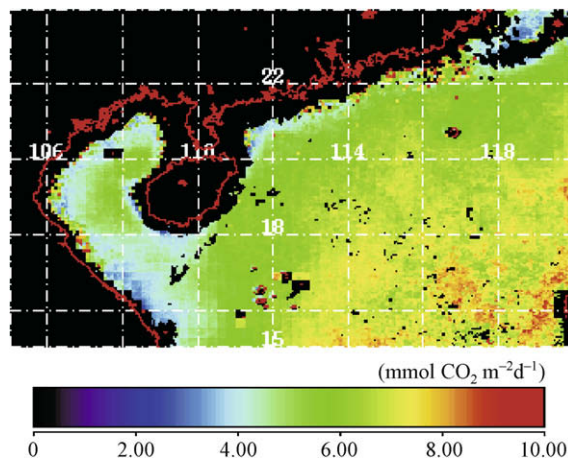


Fig. 4. Distribution of satellite-derived air–sea CO<sub>2</sub> flux in the northern South China Sea in summer (2000–2005 mean).

northern SCS were estimated based on the extrapolation of data from sporadic transects and/or time-series station observations. However, it is worth bearing in mind that this study used *in situ* data from only two cruises, one for algorithm tuning and the other for validation. In order to reduce the uncertainty in the carbon budget, it is suggested that a further investigation should be carried out based on a pool of *in situ* CO<sub>2</sub> data covering various temporal and spatial scales.

## 6. Conclusion

Satellite remote-sensing data and an SST-Chl  $a$ -dependent algorithm were used to estimate the sea surface  $p\text{CO}_2$  in the northern SCS. The results agreed well with the historical field measurements, suggesting that the remote-sensing technique is applicable to air–sea CO<sub>2</sub> flux observations in the SCS. The collection of more *in situ* data covering various temporal and spatial scales is necessary in order to improve the algorithm.

It should be noted that this paper is limited to the preliminary results for the northern SCS in the summer season. Whether this is applicable to other regions of the SCS and for other seasons requires further investigation.

## Acknowledgements

This work was supported jointly by the National Basic Research Program of China (Grant Nos. 2009CB421200 and 2009CB421201), National Natural Science Foundation of China (Grant Nos. 40521003 and 90711005), High-Tech R&D Program of China (Grant Nos. 2006AA09A302 and 2007AA09Z127). We thank Zhaozhang Chen and Caiyun Zhang for their assistance with the CTD data collection and/or processing. Wuqi Ruan and Fan Zhang along with the crew of the R/V Yanping II provided much help during the sampling cruises. We also thank Prof. John Hodgkiss for his help in the English writing of this manuscript.

## References

- [1] Takahashi T, Olafsson J, Goddard JG. Seasonal variation of CO<sub>2</sub> and nutrients in the high-latitude surface: a comparative study. *Global Biogeochem Cy* 1993;7:843–78.
- [2] Ono T, Saino T, Kurita N, et al. Basin-scale extrapolation of shipboard pCO<sub>2</sub> data by using satellite SST and Chl *a*. *Int J Remote Sens* 2004;25:3803–15.
- [3] Lohrenz SE, Cai WJ. Satellite ocean color assessment of air–sea fluxes of CO<sub>2</sub> in a river-dominated coastal margin. *Geophys Res Lett* 2006;33:11.
- [4] Stephens MP, Samuels G, Olson DB, et al. Sea–air flux of CO<sub>2</sub> in the North Pacific using shipboard and satellite data. *J Geophys Res* 1995;100:13571–83.
- [5] Sarma V, Saino T, Sasaoka K, et al. Basin-scale pCO<sub>2</sub> distribution using satellite sea surface temperature, Chl *a*, and climatological salinity in the North Pacific in spring and summer. *Global Biogeochem Cy* 2006;20. doi:10.1029/2005GB002594.
- [6] Cai WJ, Dai MH. Comment on “Enhanced open ocean storage of CO<sub>2</sub> from shelf sea pumping”. *Science* 2004;306:1477C.
- [7] Zhai WD, Dai MH, Cai WJ, et al. The partial pressure of carbon dioxide and air–sea fluxes in the northern South China Sea in spring, summer and autumn. *Mar Chem* 2005;96:87–97.
- [8] Xu XZ. Comprehensive investigation report in South China Sea. Beijing: Ocean Press; 1982, p. 119–28.
- [9] Longhurst A, Sathyendranath S, Platt T, et al. An estimate of global primary production in the ocean from satellite radiometer data. *J Plankton Res* 1995;17:1245–71.
- [10] Liss PS. Process of gas exchange across an air–water interface. *Deep-Sea Res* 1973;20:2003–23.
- [11] Weiss RF. Carbon dioxide in water and seawater: the solubility of a non-ideal gas. *Mar Chem* 1974;2:213–5.
- [12] Wanninkhof R. Relationship between wind speed and gas exchange over the ocean. *J Geophys Res* 1992;97:7373–82.
- [13] Zeebe RE, Wolf-Gladrow D. CO<sub>2</sub> in seawater: equilibrium, kinetics, isotopes. Amsterdam: Elsevier; 2001.